Physics Letters B 811 (2020) 135935

Contents lists available at ScienceDirect

Physics Letters B

www.elsevier.com/locate/physletb

$d^*(2380)$ dibaryon from lattice QCD

HAL QCD Collaboration

Shinya Gongyo [a,b,*], Kenji Sasaki [c,a], Takaya Miyamoto [a], Sinya Aoki [c,d,a], Takumi Doi [a,b], Tetsuo Hatsuda [b], Yoichi Ikeda [e,a], Takashi Inoue [f,a], Noriyoshi Ishii [g,a]

[a] Quantum Hadron Physics Laboratory, RIKEN, Saitama 351-0198, Japan
[b] iTHEMS Program, RIKEN, Saitama 351-0198, Japan
[c] Center for Gravitational Physics, Yukawa Institute for Theoretical Physics, Kyoto University, Kyoto 606-8502, Japan
[d] Center for Computational Sciences, University of Tsukuba, Ibaraki 305-8571, Japan
[e] Department of Physics, Kyushu University, Fukuoka 819-0395, Japan
[f] College of Bioresource Science, Nihon University, Kanagawa 252-0880, Japan
[g] Research Center for Nuclear Physics (RCNP), Osaka University, Osaka 567-0047, Japan

ARTICLE INFO

Article history:
Received 9 June 2020
Received in revised form 31 October 2020
Accepted 4 November 2020
Available online 10 November 2020
Editor: J.-P. Blaizot

Keywords:
Lattice QCD
Decuplet baryons
ABC effect
$d^*(2380)$

ABSTRACT

The $\Delta\Delta$ dibaryon resonance $d^*(2380)$ with $(J^P, I) = (3^+, 0)$ is studied theoretically on the basis of the 3-flavor lattice QCD simulation with heavy pion masses ($m_\pi = 679, 841$ and 1018 MeV). By using the HAL QCD method, the central Δ-Δ potential in the $^7S_3$ channel is obtained from the lattice data with the lattice spacing $a \simeq 0.121$ fm and the lattice size $L \simeq 3.87$ fm. The resultant potential shows a strong short-range attraction, so that a quasi-bound state corresponding to $d^*(2380)$ is formed with the binding energy 25-40 MeV below the $\Delta\Delta$ threshold for the heavy pion masses. The tensor part of the transition potential from $\Delta\Delta$ to NN is also extracted to investigate the coupling strength between the S-wave $\Delta\Delta$ system with $J^P = 3^+$ and the D-wave NN system. Although the transition potential is strong at short distances, the decay width of $d^*(2380)$ to NN in the D-wave is kinematically suppressed, which justifies our single-channel analysis at the range of the pion mass explored in this study.

1. Introduction

Recently much interest has been attracted to decuplet-decuplet dibaryons as well as to octet-octet and octet-decuplet dibaryons [1–8]. Theoretically, the quark Pauli principle provides an important guideline to identify possible dibaryon channels [9,10]: If the overlap of the quark wave functions is forbidden by the quark Pauli principle, it is difficult to form dibaryons, while if the overlap is allowed or only partially forbidden, there is a chance.

To see the role of quark Pauli principle more explicitly in the decuplet-decuplet system, let us consider its irreducible representation of the SU(3) flavor symmetry,

$$\mathbf{10} \otimes \mathbf{10} = (\mathbf{28} \oplus \mathbf{27})_{\text{sym.}} \oplus (\mathbf{35} \oplus \mathbf{10}^*)_{\text{anti-sym.}},$$

where "sym." and "anti-sym." stand for the flavor symmetry under the exchange of two baryons. Then one finds that there are two Pauli-allowed S-wave states: Spin 0 in symmetric **28** representation and spin 3 in anti-symmetric $\mathbf{10}^*$ representation. The $\Omega\Omega$ system in the spin-0 channel belongs to the former, while the $\Delta\Delta$ system in the spin-3 and isospin-0 channel belongs to the latter [11]. In fact, these two systems have been studied extensively by using phenomenological models (see e.g. [12–15] for the $\Omega\Omega$, and [16–19] for the $\Delta\Delta$). Only recently, the first principle lattice QCD simulation of the baryon-baryon interactions near the physical point became possible thanks to the HAL QCD method, and it was shown that the $\Omega\Omega$ interaction in the spin-0 channel supports a shallow dibaryon state, the di-Omega, near unitarity [3]. It is also proposed to search for such a state by the momentum correlation of Ω-pairs in future heavy-ion collision experiments [6].

As for the $\Delta\Delta$ system, a dibaryon with spin-3 and isospin-0 has been reported experimentally [20,21]. It is now called $d^*(2380)$ and has a resonance peak about 80 MeV below the $\Delta\Delta$ threshold with the total width $\Gamma \simeq 70$ MeV. The recent exclusive experiment has revealed its detailed properties such as the branching ratios into NN, $NN\pi$, and $NN\pi\pi$ [2,22]. Thus it is highly desirable to make a first principle lattice QCD calculation of $d^*(2380)$. However,

* Corresponding author.
E-mail address: shinya.gongyo@riken.jp (S. Gongyo).

https://doi.org/10.1016/j.physletb.2020.135935
0370-2693/

it is a much involved task in comparison to di-Omega primarily because $d^*(2380)$ is a resonance above multi-particle thresholds such as $NN\pi$ and $NN\pi\pi$. Instead of studying the problem with extensive coupled-channel approach on the lattice, we take heavy quark masses to capture the essential mechanism of the formation of $d^*(2380)$ from two Δs. In such a lattice setup, Δ becomes a stable particle without decaying into $N\pi$ and $d^*(2380)$ may appear as a spin-3 and S-wave quasi-bound state of $\Delta\Delta$ which can decay to NN only through the D-wave and the G-wave. Such a lattice result not only reveals the physics behind $d^*(2380)$ but also provides useful input to the effective field theory approach toward the physical point [23].

This paper is organized as follows. In Sec. 2, we introduce the HAL QCD method to extract the Δ-Δ central potential from lattice QCD. In Sec. 3, we summarize setup of our lattice QCD simulations. In Sec. 4, we show the numerical results of Δ-Δ central potential in $^7S_3$ channel. Sec. 5 is devoted to summary. In Appendix A, we show the transition potential from $\Delta\Delta$ to NN and estimate the decay rate to be small, which justifies the single-channel approach.

2. HAL QCD method for $\Delta\Delta$ interaction

In QCD, the $\Delta\Delta$ potential in the $^7S_3$ channel is obtained from the equal-time Nambu-Bethe-Salpeter (NBS) wave function defined by

$$\psi_n^{\Delta\Delta}(\vec{r}) = \langle 0|\,[\Delta\Delta]^{(s=3,I=0)}\,(\vec{r},0)\,|W_n;\,J=3,I=0\rangle\,, \tag{1}$$

where $|W_n;\,J=3,I=0\rangle$ stands for a QCD eigenstate which has the total energy $W_n = 2\sqrt{k_n^2+m_\Delta^2}$ with m_Δ being Δ-baryon's mass, the total spin J=3 and the isospin I=0. $[\Delta\Delta]^{(s=3,I=0)}\,(\vec{r},t)$= $\sum_{\alpha,\beta,l,m,A,B,\vec{x}} P^{(s=3,I=0)}_{\alpha,\beta,l,m,A,B}\Delta^A_{\alpha,l}(\vec{x}+\vec{r},t)\Delta^B_{\beta,m}(\vec{x},t)$ is a two Δ-baryon operator with $P^{(s=3,I=0)}_{\alpha,\beta,l,m,A,B}$ being the projection operator onto the internal spin $s=3$ and $I=0$. The Δ-baryon operator $\Delta^A_{\alpha,l}(\vec{x}+\vec{r})$ with the charge index A, the spinor index α, and the Lorentz index l is constructed from the liner combinations of interpolating operators, $\epsilon^{abc}q_a^T(x)C\gamma_l q_b(x)q_{c\alpha}(x)$ with $q=u,d$ and $C\equiv\gamma_4\gamma_2$.

We first assume that the couplings of $\Delta\Delta(^7S_3)$ to the D-wave and the G-wave NN states below the $\Delta\Delta$ threshold is small and consider the single channel analysis between Δs. Justification of this assumption will be discussed in Appendix A.

Since the NBS wave function in the asymptotically large distance is identical to that of the scattering state or bound state in 2-body quantum mechanics [24,25], one can define the $\Delta\Delta$ potential via the Schrödinger-type equation obtained from the equal-time NBS equation as [26]:

$$\begin{aligned}&-\frac{\nabla^2}{m_\Delta}\psi_n^{\Delta\Delta}(\vec{r}) + \int U^{\Delta\Delta}(\vec{r},\vec{r}\,')\psi_n^{\Delta\Delta}(\vec{r}\,')d^3\vec{r}\,' \\ &= E_n\psi_n^{\Delta\Delta}(\vec{r}),\end{aligned} \tag{2}$$

with m_Δ being the mass of Δ and $E_n = k_n^2/m_\Delta$. Note that the non-local potential $U^{\Delta\Delta}(\vec{r},\vec{r}\,')$ is energy-independent. The NBS wave function is related to the reduced four-point function,

$$\begin{aligned}R^{\Delta\Delta}_{J=3}(\vec{r},t) &= \langle 0|\,[\Delta\Delta]^{(s=3,I=0)}\,(\vec{r},t)\,\bar{\mathcal{J}}^{J=3}_{\Delta\Delta}(0)\,|0\rangle\,/e^{-2m_\Delta t} \\ &= \sum_n a_n\psi_n^{\Delta\Delta}(\vec{r})e^{-\delta W_n t} + O(e^{-\Delta E^*\cdot t})\end{aligned} \tag{3}$$

with $a_n = \langle W_n;\,J=3,I=0|\,\bar{\mathcal{J}}^{J=3}_{\Delta\Delta}(0)\,|0\rangle$, $\delta W_n = W_n - 2m_\Delta$, $\Delta E^*(>0)$ being the energy difference between the inelastic threshold and $2m_\Delta$, and $\bar{\mathcal{J}}^{J=3}_{\Delta\Delta}(0)$ being a source operator with $J=3$.

Below the inelastic threshold, $R^{\Delta\Delta}_{J=3}(\vec{r},t)$ satisfies the time-dependent HAL QCD equation [27],

$$\begin{aligned}&\left(\frac{\nabla^2}{m_\Delta} - \frac{\partial}{\partial t} + \frac{1}{4m_\Delta}\frac{\partial^2}{\partial t^2}\right)R^{\Delta\Delta}_{J=3}(\vec{r},t) \\ &\quad= \int U^{\Delta\Delta}(\vec{r},\vec{r}\,')R^{\Delta\Delta}_{J=3}(\vec{r}\,',t)d\vec{r}\,'.\end{aligned} \tag{4}$$

Using the derivative expansion of the non-local potential, $U^{\Delta\Delta}(\vec{r},\vec{r}\,') = V^{\Delta\Delta}(\vec{r})\delta(\vec{r}-\vec{r}\,') + O(\vec{\nabla})$, the leading-order (LO) local potential can be obtained as

$$V^{\Delta\Delta}(\vec{r}) = \left[R^{\Delta\Delta}_{J=3}(\vec{r},t)\right]^{-1}\left(\frac{\nabla^2}{m_\Delta} - \frac{\partial}{\partial t} + \frac{1}{4m_\Delta}\frac{\partial^2}{\partial t^2}\right)R^{\Delta\Delta}_{J=3}(\vec{r},t). \tag{5}$$

The resultant potential can then be used to calculate the observables such as the binding energy and the phase shift in the infinite volume.[1]

The systematic error in Eq. (5) originating from the LO truncation of the derivative expansion can be estimated from the residual time-dependence of $V^{\Delta\Delta}(\vec{r})$. Also, the higher-order terms can be determined by using the multiple source functions for $\bar{\mathcal{J}}^{J=3}_{\Delta\Delta}$. It was shown in [31,33] that the next-to-LO potential obtained by combining a wall source and a smeared source for a two-octet baryon system gives negligible effects to physical observable at low energies for heavy pion masses.

3. Simulation setup

We employ the full QCD gauge configurations in the flavor-$SU(3)$ limit with the renormalization-group improved gauge action and the non-perturbatively $O(a)$ improved Wilson quark action at $\beta=1.83$ and $\kappa_{uds}=0.13710, 0.13760, 0.13800$ for $32^3\times 32$ lattice. The lattice spacing a and the physical volume correspond to 0.121 fm and $(3.87\text{ fm})^3$, respectively. We have used 360 configurations for $\kappa_{uds}=0.13710, 0.13800$ and 480 configurations for $\kappa_{uds}=0.13760$ given in Ref. [10]. The wall-type quark source with the Coulomb gauge fixing is employed.

To increase the statistics, the forward and backward propagations are averaged and the rotational symmetry on the lattice (4 rotations) and the translational invariance for the source position (32 temporal positions) are utilized for each configuration. The hadron masses obtained by the single exponential fit are summarized in Table 1. The statistical errors are estimated by the Jackknife method with 18 samples for $\kappa_{uds}=0.13710, 0.13800$ and 24 samples for $\kappa_{uds}=0.13760$. The fit results are slightly different from Ref. [10], because we use more statistics and different fit ranges. In all cases, m_Δ is below the threshold, $m_\pi+m_N$, so that Δ is a stable baryon.

Table 1
The hadron masses obtained from the single exponential fit in the intervals, $t/a = 6-11$ (pion) and $t/a = 7-12$ (baryons).

κ_{uds}	m_π [MeV]	m_N [MeV]	m_Δ [MeV]
0.13710	1017.5(2)	2019.4(5)	2213.6(7)
0.13760	840.6(2)	1739.1(5)	1940.3(6)
0.13800	679.0(2)	1476.9(5)	1676.9(8)

[1] We have observed that if one applies Lüscher's finite volume analysis [28] without a variational method, the plateaux of the two-baryon spectrum are achieved at physically unrealizable time and therefore are plagued by unresolved systematic uncertainties [29–31]. Recent results on the two-nucleon system by using the Lüscher's finite volume analysis with the variational method [32] support this view independently. Therefore, we only report results with the HAL QCD method in this paper.

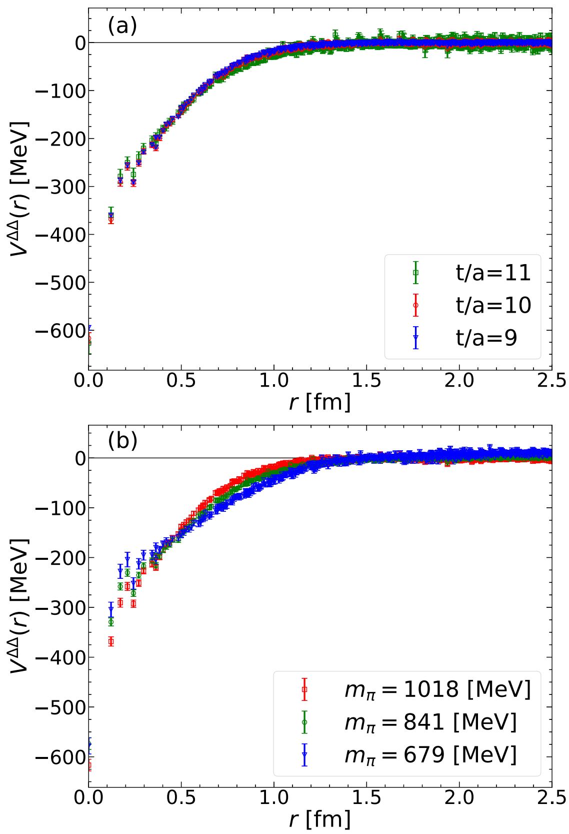

Fig. 1. The $\Delta\Delta$ central potential $V^{\Delta\Delta}(r)$ in the $^7S_3$ channel. (a) Results at $t/a = 9, 10, 11$ and $m_\pi = 1018$ MeV. (b) Results at $m_\pi = 1018$ MeV, 841 MeV, 679 MeV and $t/a = 10$.

4. $\Delta\Delta$ potential, phase shift, and binding energy

Shown in Fig. 1 are the central potentials in the $^7S_3$ channel $V^{\Delta\Delta}(r)$ as a function of r in the range $t/a = 9, 10, 11$ and $m_\pi = 679, 841, 1018$ MeV. As seen from Fig. 1 (a), $V^{\Delta\Delta}(r)$ for different t are nearly identical within the statistical errors indicating that the contribution from higher-order potential is not relevant. We also find that $V^{\Delta\Delta}(r)$ is attractive for the whole distance.[2] The long-range part of the attraction becomes stronger as m_π decreases as seen from Fig. 1(b). These features can be understood by (i) the absence of Pauli exclusion effect for quarks in this channel, (ii) the absence of the color magnetic effect in one-gluon exchange at short distance [9], and (iii) the attractive one-pion exchange at long distance. We perform uncorrelated fit for the lattice data of the $\Delta\Delta$ potential in the range $r = 0 - 1.5$ fm by two Gaussians plus one Yukawa form with a form factor as

$$V^{\Delta\Delta}(\vec{r}) = b_1 e^{-(\frac{r}{b_2})^2} + b_3 e^{-(\frac{r}{b_4})^2} + b_5(1 - e^{-(\frac{r}{b_6})^2})\frac{e^{-m_\pi r}}{r}. \quad (6)$$

For example, the fitting at $m_\pi = 679$ MeV and $t/a = 10$ results in $b_1 = -457(29)$ MeV, $b_2 = 0.090(4)$ fm, $b_3 = -121(31)$ MeV, $b_4 = 0.15(2)$ fm, $b_5 = -1924(533)$ MeV $\cdot$ fm, $b_6 = 0.98(16)$ fm, with $\chi^2/\text{dof} \simeq 1$. The systematic errors in the fitting form are negligible in comparison with statistical errors and systematic errors from the t dependence.

[2] None-smooth behavior of the potential at $r < 0.2$ fm originates most likely from the lattice discretization: To remove the error, we need to take the continuum limit by collecting the data for different lattice spacings.

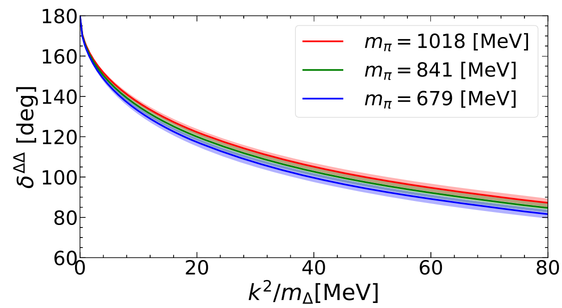

Fig. 2. The phase shift $\delta^{\Delta\Delta}$ in the $\Delta\Delta(^7S_3)$ channel as a function of k^2/m_Δ for three pion masses.

Using the fitted potential and solving the Schrödinger equation in the infinite volume, we obtain the hypothetical $\Delta\Delta$ scattering phase shift $\delta^{\Delta\Delta}$ in the $^7S_3$ channel as a function of k^2/m_Δ in Fig. 2 for three different pion masses. In all three cases, the phase shift starts from 180° at $k^2 = 0$, indicating the presence of a quasi-bound state in the $\Delta\Delta(^7S_3)$ channel.

The binding energy $B_{\Delta\Delta}$ can be also obtained from the Schrödinger equation. The results of the bound state energy $E_0 = -B_{\Delta\Delta}$ for different t/a and m_π are shown in Fig. 3(a). Also shown in Fig. 3(b) are the bound state energy E_0 and the root-mean-square distance $\sqrt{\langle r^2\rangle_{\Delta\Delta}}$ of the $\Delta\Delta$ quasi-bound state. The typical size of the quasi-bound state is 0.8–1 fm and the final values of the binding energies read

$$\begin{aligned} m_\pi &= 1018\text{ MeV}: \ B_{\Delta\Delta} = 37.4(3.3)(^{+1.2}_{-0.4})\text{ MeV}, \\ m_\pi &= 841\text{ MeV}: \ B_{\Delta\Delta} = 33.6(3.7)(^{+1.8}_{-1.7})\text{ MeV}, \\ m_\pi &= 679\text{ MeV}: \ B_{\Delta\Delta} = 29.8(3.4)(^{+6.7}_{-5.0})\text{ MeV}, \end{aligned} \quad (7)$$

with the statistical errors (first) and systematic errors from the t dependence (second).

5. Summary

We have studied the $\Delta\Delta$ system in the $(J, I) = (3, 0)$ channel, where the resonant dibaryon $d^*(2380)$ was observed, from the lattice QCD simulation with heavy quark masses in the flavor-$SU(3)$ limit. The Δ-Δ central potential in the $^7S_3$ channel calculated by the HAL QCD method is found to be attractive in all distance. The phase shifts obtained by solving the Schrödinger equation using the potential show the presence of the deep quasi-bound state below the $\Delta\Delta$ threshold. The energy below the threshold is estimated from $t/a = 10$ to be about 30 MeV in the case of the lightest pion mass $m_\pi = 679$ MeV.

Our result implies that other members of **10*** representation such as $\Delta\Sigma^*$ in the $(J, I) = (3, 1/2)$ channel and $\Delta\Xi^*$ in the $(J, I) = (3, 1)$ channel may have dibaryons due to the similar central attraction shown in the $\Delta\Delta$ system. However, the systems are more intricate even with heavy quark masses, because of their decay not only into octet-octet systems but also into octet-decuplet systems through D and G waves.

The lattice simulation of the $\Delta\Delta$ system near the physical point is left for future studies. Since Δ baryon can decay into $N\pi$, the $\Delta\Delta$ system can also decay into $NN\pi$ and $NN\pi\pi$ as well as NN. Therefore, the coupled channel equations associated with three and four hadron systems, which is challenging not only in the simulation but also in the formulation on the lattice [34], are needed to extract potentials.

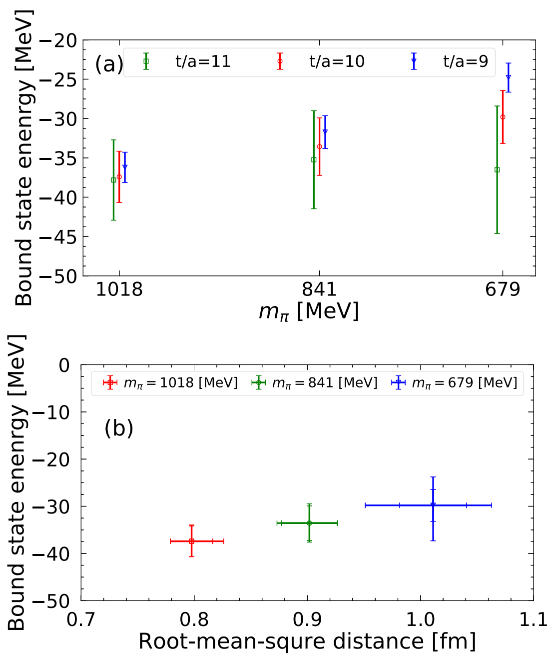

Fig. 3. (a) Bound state energy in the $\Delta\Delta(^7S_3)$ channel at $t/a = 9, 10, 11$ and $m_\pi = 1018$ MeV, 841 MeV, 679 MeV. (b) Bound state energy and the root-mean-square distance at $t/a = 10$ and $m_\pi = 1018$ MeV, 841 MeV, 679 MeV. Inner bars correspond to the statistical errors, while the outer bars are obtained by the quadrature of the statistical and systematic errors estimated from the central values for $t/a = 9, 11$.

Declaration of competing interest

The authors declare that they have no known competing financial interests or personal relationships that could have appeared to influence the work reported in this paper.

Acknowledgement

S.G. was supported by the Special Postdoctoral Researchers Program of RIKEN and iTHEMS Program. The authors thank K. Yazaki and T. Abe for fruitful discussions on the $\Delta\Delta$ system and its transition potential to NN system. T.H., S.A. and T.D. was partially supported by JSPS Grant No. JP18H05236. S.A. was partially supported by JSPS Grant No. JP16H03978. T.D. was partially supported by JSPS Grant No. JP19K03879 and JP18H05407. The lattice QCD calculations have been performed on HOKUSAI supercomputers at RIKEN. This work was partially supported by "Priority Issue on Post-K computer" (Elucidation of the Fundamental Laws and Evolution of the Universe), "Program for Promoting Researches on the Supercomputer Fugaku" (Simulation for basic science: from fundamental laws of particles to creation of nuclei) and Joint Institute for Computational Fundamental Science (JICFuS).

Appendix A. Transition from $\Delta\Delta$ to NN

The threshold of the NN system ($J = 3$) in higher partial waves, $^3D_3$ and $^3G_3$, are below the quasi-bound state of $\Delta\Delta$ system. In the main text, we have neglected such transition and derived the single-channel $\Delta\Delta$ potential in the S-wave. To estimate the magnitude of the decay rate from the quasi-bound state to the NN scattering states, let us calculate the transition potential $V^{NN;\Delta\Delta}(\vec{r})$ by using the general operator form in $I = 0$ [35,36],

$$V^{NN;NN}(\vec{r}) = V_0^{NN;NN}(r) + V_\sigma^{NN;NN}(r)\vec{\sigma}_1\cdot\vec{\sigma}_2 + V_T^{NN;NN}(r)S_{12}^\sigma$$

$$V^{NN;\Delta\Delta}(\vec{r}) = V_S^{NN;\Delta\Delta}(r)\vec{S}_1\cdot\vec{S}_2 + V_T^{NN;\Delta\Delta}(r)S_{12}^S, \tag{A.1}$$

where $\vec{S}_i (i = 1, 2)$ is the transition operator from the spin-3/2 state to the spin-1/2 state,[3] and S_{12}^A $(A = \sigma, S)$ is the tensor operator associated with $\vec{\sigma}$ and $\vec{S}$, respectively:

$$S_{12}^A \equiv 3\frac{\left(\vec{A}_1\cdot\vec{r}\right)\left(\vec{A}_2\cdot\vec{r}\right)}{r^2} - \vec{A}_1\cdot\vec{A}_2. \tag{A.2}$$

For NN system with $s = 1$ and $I = 0$, we have $\vec{\sigma}_1\cdot\vec{\sigma}_2 = 1$, so that $V_0^{NN;NN}(r)$ and $V_\sigma^{NN;NN}(r)\vec{\sigma}_1\cdot\vec{\sigma}_2$ are combined into

$$V_C^{NN;NN}(r) \equiv V_0^{NN;NN}(r) + V_\sigma^{NN;NN}(r). \tag{A.3}$$

The potentials, $V^{NN;NN}(r)$ and $V^{NN;\Delta\Delta}(r)$, appear in the coupled channel equations between NN and $\Delta\Delta$ [34]

$$\left(\frac{\nabla^2}{m_N} - \frac{\partial}{\partial t} + \frac{1}{4m_N}\frac{\partial^2}{\partial t^2}\right)R_J^{NN}(\vec{r}, t) = V^{NN;\Delta\Delta}(\vec{r})R_J^{\Delta\Delta}(\vec{r}, t) + V^{NN;NN}(\vec{r})R_J^{NN}(\vec{r}, t), \tag{A.4}$$

where $R_J^{NN}(\vec{r}, t)$ is given by

$$R_J^{NN}(\vec{r}, t) = \langle 0| [NN]_J^{(s=1,I=0)}(\vec{r}, t)\bar{\mathcal{J}}_{\Delta\Delta}^{(s',I=0)}(0)|0\rangle / e^{-2m_N t}, \tag{A.5}$$

with $[NN]_J^{(s=1,I=0)}(\vec{r}, t)$ being the NN operator with $s = 1$, $I = 0$, and $J = 1, 3$, and $\bar{\mathcal{J}}_{\Delta\Delta}^{(s',I=0)}(0)$ being the $\Delta\Delta$ source operator constructed from wall-type quark source with internal spin $s' = J$. $R_J^{\Delta\Delta}(\vec{r}, t)$ is defined to include the wave function renormalization factor (Z-factor) and the kinetic correction factor to compensate the threshold energy difference between $\Delta\Delta$ and NN [37,5].

To extract the potentials from Eq. (A.4), we have to utilize $R_J^{NN}(\vec{r}, t)$ and $R_J^{\Delta\Delta}(\vec{r}, t)$ with given J. Since our $\Delta\Delta$ source operator with internal spin s' is invariant under the A_1^+ projection, it contains not only $l = 0$ but also $l \geq 4$. Therefore, it couples to the multiple total angular momenta, $J = s', |s' - 4|, |s' - 4| + 1, \ldots$. To construct the NN-$\Delta\Delta$ correlation with given J, we employ the Misner's projection, where each (l, l_z) contribution can be obtained separately by using points inside the shell that are not connected with each other under the cubic transformation [38,39]. For the sink operator with the internal spin s, we perform the (l, l_z) projection by Misner's method and have constructed J-projection using appropriate Clebsch-Gordan coefficients.

In principle, we can determine the four potentials, $V_C^{NN;NN}(r)$, $V_T^{NN;NN}(r)$, $V_S^{NN;\Delta\Delta}(r)$, and $V_T^{NN;\Delta\Delta}(r)$, from the four independent equations obtained by the projection of (A.4) into $l = 0$ (S-wave) and $l = 2$ (D-wave) components in $J = 1$ and $l = 2$ (D-wave) and $l = 4$ (G-wave) components in $J = 3$. In practice, however, due to large statistical fluctuations of the $l = 4$ component, we cannot determine them precisely.

Alternatively, by assuming that the spin-spin part of the transition potential, $V_S^{NN;\Delta\Delta}(r)\vec{S}_1\cdot\vec{S}_2$, which cannot make the transition from S-wave to higher partial waves, is negligibly small, we have extracted the remnant three potentials from the $l = 0$ and $l = 2$ components in $J = 1$ and the $l = 2$ component in $J = 3$. Again, we have used Misner's projection.

Shown in Fig. 4(a)–(c) are the quark mass dependence of the three potentials, $V_C^{NN;NN}(r)$, $V_T^{NN;NN}(r)$, $V_T^{NN;\Delta\Delta}(r)$, at $t/a = 10$. In Fig. 4(a)–(b), we observe that the central potential $V_C^{NN;NN}(r)$ and the tensor potential $V_T^{NN;NN}(r)$ show the qualitatively similar behavior of the phenomenologically well-known potential in the spin-triplet channel of NN system: the short-range repulsion and

[3] The definition of $\vec{S}$ corresponds to that of $\vec{S}^\dagger$ in Ref. [35].

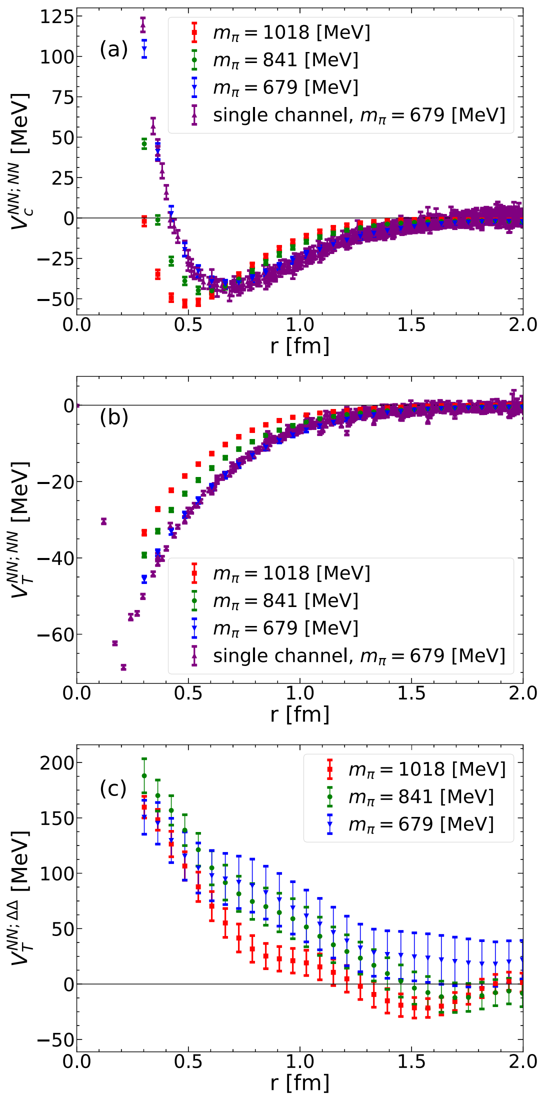

Fig. 4. The central part $V_C^{NN;NN}(r)$ and the tensor part $V_T^{NN;NN}(r)$ of the diagonal potential in NN system and the tensor part of the transition potential $V_T^{NN;\Delta\Delta}(r)$ from $\Delta\Delta$ to NN at $\kappa_{uds} = 0.13710, 0.13760, 0.13800$ corresponding to $m_\pi = 1018$ MeV, 841 MeV, 679 MeV, and $t/a = 10$. The single channel results for the central potential and the tensor potential at $\kappa_{uds} = 0.13800$ obtained by using NN source in the conventional method are taken from Ref. [10].

the intermediate-range and long-range attraction for the central potential and the all-range negative tensor potential. Furthermore, we find that all the results obtained by the coupled channel equations using $\Delta\Delta$ sources in $J = 1$ and $J = 3$ are nearly identical with the previous results obtained by the single-channel equation using NN source in $J = 1$ [40,10]. In Fig. 4(a)–(b), we also show the results from the single-channel equation at $\kappa_{uds} = 0.13800$ corresponding to $m_\pi = 679$ MeV, taken from Ref. [10] (where $m_\pi = 672$ MeV is quoted due to the different statistics and fit-range). This good agreement implies that the analysis of the three potentials by neglecting the spin-spin part of the transition potential works well.[4]

In Fig. 4(c), we find that the tensor part of the transition potential increases significantly as r decreases for all the quark masses, while it has relatively large statistical errors compared with the other potentials. Using the transition potential, we then have estimated the decay rate at $J = 3$ from the quasi-bound state of the $\Delta\Delta$ system in the S-wave to NN in the D-wave given by

$$\Gamma \simeq \int \frac{d^3k_1}{(2\pi)^3} \int \frac{d^3k_2}{(2\pi)^3} (2\pi)^4 \delta^4(k_1^\mu + k_2^\mu - K^\mu) \times \frac{6}{5} \left| \int r^2 dr \bar{\psi}^{NN}_{^3D_3}(r) V_T^{NN;\Delta\Delta}(r) \bar{\psi}^{\Delta\Delta}_{^7S_3}(r) \right|^2 \tag{A.6}$$

with $K^\mu \simeq (2m_\Delta - B_{\Delta\Delta}, \mathbf{0})$ and $\bar{\psi}^{NN}_{^3D_3}(r)$ and $\bar{\psi}^{\Delta\Delta}_{^7S_3}(r)$ being radial wave function of NN scattering state in $^3D_3$ channel and that of the $\Delta\Delta$ quasi-bound state in $^7S_3$ channel, respectively. Here, we have used the transition potential at $t/a = 10$ by fitting the two r-Gaussian form, $V_T^{NN;\Delta\Delta}(r) = \sum_{i=1}^2 p_i r \exp\left[-(r/q_i)^2\right]$ with fitting parameters p_i, q_i $(i = 1, 2)$, and the $\Delta\Delta$ wave function by solving the Schrödinger equation using the central potential at $t/a = 10$. For the sake of simplicity, we have employed the free radial wave function for the NN scattering state, $\bar{\psi}^{NN}_{^3D_3}(r) = -\sqrt{10\pi}\, j_2(kr)$, with $j_2(kr)$ being the spherical Bessel function of order two. This results in $\Gamma = (1.6(6)$ MeV, $5.6(1.7)$ MeV, $6.4(1.8)$ MeV) for $m_\pi = (1018$ MeV, 841 MeV, 679 MeV). Due to the repulsive interaction, the wave function for the NN scattering state in higher partial waves becomes smaller at short distances, only where the transition potential becomes non-negligible. Therefore, the decay rate is further reduced if more realistic wave function is employed.

[4] Having neglected the tensor part instead of the spin-spin part, the obtained central potential and tensor potential in NN system are completely different from the previous results in Ref. [10]. Even the short-range repulsion cannot be found.

References

[1] A. Gal, Meson assisted dibaryons, Acta Phys. Pol. B 47 (2016) 471, https://doi.org/10.5506/APhysPolB.47.471, arXiv:1511.06605.
[2] H. Clement, On the history of dibaryons and their final observation, Prog. Part. Nucl. Phys. 93 (2017) 195, https://doi.org/10.1016/j.ppnp.2016.12.004, arXiv:1610.05591.
[3] S. Gongyo, et al., Most strange dibaryon from lattice QCD, Phys. Rev. Lett. 120 (2018) 212001, https://doi.org/10.1103/PhysRevLett.120.212001, arXiv:1709.00654.
[4] T. Iritani, et al., $N\Omega$ dibaryon from lattice QCD near the physical point, Phys. Lett. B 792 (2019) 284–289, https://doi.org/10.1016/j.physletb.2019.03.050, arXiv:1810.03416.
[5] K. Sasaki, et al., $\Lambda\Lambda$ and $N\Xi$ interactions from lattice QCD near the physical point, Nucl. Phys. A (2019) 121737, https://doi.org/10.1016/j.nuclphysa.2020.121737, arXiv:1912.08630.
[6] K. Morita, S. Gongyo, T. Hatsuda, T. Hyodo, Y. Kamiya, A. Ohnishi, Probing $\Omega\Omega$ and $p\Omega$ dibaryons with femtoscopic correlations in relativistic heavy-ion collisions, Phys. Rev. C 101 (1) (2020) 015201, https://doi.org/10.1103/PhysRevC.101.015201, arXiv:1908.05414.
[7] L. Tolos, L. Fabbietti, Strangeness in nuclei and neutron stars, Prog. Part. Nucl. Phys. 112 (2020) 103770, https://doi.org/10.1016/j.ppnp.2020.103770.
[8] S. Aoki, T. Doi, Lattice QCD and baryon-baryon interactions: HAL QCD method, Front. Phys. 8 (2020) 307, https://doi.org/10.3389/fphy.2020.00307, arXiv:2003.10730.
[9] M. Oka, K. Shimizu, K. Yazaki, Quark cluster model of baryon baryon interaction, Prog. Theor. Phys. Suppl. 137 (2000) 1–20, https://doi.org/10.1143/PTPS.137.1.
[10] T. Inoue, S. Aoki, T. Doi, T. Hatsuda, Y. Ikeda, N. Ishii, K. Murano, H. Nemura, K. Sasaki, Two-baryon potentials and H-dibaryon from 3-flavor lattice QCD simulations, Nucl. Phys. A 881 (2012) 28–43, https://doi.org/10.1016/j.nuclphysa.2012.02.008, arXiv:1112.5926.
[11] F. Dyson, N.H. Xuong, Y=2 states in Su(6) theory, Phys. Rev. Lett. 13 (26) (1964) 815–817, https://doi.org/10.1103/PhysRevLett.13.815.
[12] Z.Y. Zhang, Y.W. Yu, P.N. Shen, L.R. Dai, A. Faessler, U. Straub, Hyperon nucleon interactions in a chiral SU(3) quark model, Nucl. Phys. A 625 (1997) 59–70, https://doi.org/10.1016/S0375-9474(97)00033-X.
[13] Z.Y. Zhang, Y.W. Yu, C.R. Ching, T.H. Ho, Z.-D. Lu, Suggesting a di-omega dibaryon search in heavy ion collision experiments, Phys. Rev. C 61 (2000) 065204, https://doi.org/10.1103/PhysRevC.61.065204.
[14] F. Wang, G.-h. Wu, L.-j. Teng, J.T. Goldman, Quark delocalization, color screening, and nuclear intermediate range attraction, Phys. Rev. Lett. 69 (1992) 2901–2904, https://doi.org/10.1103/PhysRevLett.69.2901, arXiv:nucl-th/9210002.
[15] F. Wang, J.-l. Ping, G.-h. Wu, L.-j. Teng, J.T. Goldman, Quark delocalization, color screening and dibaryons, Phys. Rev. C 51 (1995) 3411, https://doi.org/10.1103/PhysRevC.51.3411, arXiv:nucl-th/9512014.

[16] T. Kamae, T. Fujita, Possible existence of a deeply bound delta-delta system, Phys. Rev. Lett. 38 (1977) 471–475, https://doi.org/10.1103/PhysRevLett.38.471.
[17] M. Oka, K. Yazaki, Nuclear force in a quark model, Phys. Lett. B 90 (1980) 41–44, https://doi.org/10.1016/0370-2693(80)90046-5.
[18] X. Yuan, Z. Zhang, Y. Yu, P. Shen, Deltaron dibaryon structure in chiral SU(3) quark model, Phys. Rev. C 60 (1999) 045203, https://doi.org/10.1103/PhysRevC.60.045203, arXiv:nucl-th/9901069.
[19] Y. Dong, P. Shen, F. Huang, Z. Zhang, Study of $d^*(2380)$ resonance in a chiral constituent quark model, Int. J. Mod. Phys. A 33 (33) (2018) 1830031, https://doi.org/10.1142/S0217751X18300314.
[20] T. Kamae, I. Arai, T. Fujii, H. Ikeda, N. Kajiura, S. Kawabata, K. Nakamura, K. Ogawa, T. Takeda, Y. Watase, Observation of an anomalous structure in proton polarization from deuteron photodisintegration, Phys. Rev. Lett. 38 (1977) 468, https://doi.org/10.1103/PhysRevLett.38.468.
[21] P. Adlarson, et al., ABC effect in basic double-pionic fusion — observation of a new resonance?, Phys. Rev. Lett. 106 (2011) 242302, https://doi.org/10.1103/PhysRevLett.106.242302, arXiv:1104.0123.
[22] M. Bashkanov, H. Clement, T. Skorodko, Branching ratios for the decay of $d^*(2380)$, Eur. Phys. J. A 51 (7) (2015) 87, https://doi.org/10.1140/epja/i2015-15087-x, arXiv:1502.07156.
[23] J. Haidenbauer, S. Petschauer, N. Kaiser, U.-G. Meissner, W. Weise, Scattering of decuplet baryons in chiral effective field theory, Eur. Phys. J. C 77 (11) (2017) 760, https://doi.org/10.1140/epjc/s10052-017-5309-4, arXiv:1708.08071.
[24] S. Aoki, N. Ishii, T. Doi, Y. Ikeda, T. Inoue, Asymptotic behavior of Nambu-Bethe-Salpeter wave functions for multiparticles in quantum field theories, Phys. Rev. D 88 (1) (2013) 014036, https://doi.org/10.1103/PhysRevD.88.014036, arXiv:1303.2210.
[25] S. Gongyo, S. Aoki, Asymptotic behavior of Nambu-Bethe-Salpeter wave functions for scalar systems with a bound state, PTEP 2018 (9) (2018) 093B03, https://doi.org/10.1093/ptep/pty097, arXiv:1807.02967.
[26] S. Aoki, T. Hatsuda, N. Ishii, Theoretical foundation of the nuclear force in QCD and its applications to central and tensor forces in quenched lattice QCD simulations, Prog. Theor. Phys. 123 (2010) 89–128, https://doi.org/10.1143/PTP.123.89, arXiv:0909.5585.
[27] N. Ishii, S. Aoki, T. Doi, T. Hatsuda, Y. Ikeda, T. Inoue, K. Murano, H. Nemura, K. Sasaki, Hadron-hadron interactions from imaginary-time Nambu-Bethe-Salpeter wave function on the lattice, Phys. Lett. B 712 (2012) 437–441, https://doi.org/10.1016/j.physletb.2012.04.076, arXiv:1203.3642.
[28] M. Luscher, Two particle states on a torus and their relation to the scattering matrix, Nucl. Phys. B 354 (1991) 531–578, https://doi.org/10.1016/0550-3213(91)90366-6.
[29] T. Iritani, et al., Mirage in temporal correlation functions for baryon-baryon interactions in lattice QCD, J. High Energy Phys. 10 (2016) 101, https://doi.org/10.1007/JHEP10(2016)101, arXiv:1607.06371.
[30] T. Iritani, S. Aoki, T. Doi, T. Hatsuda, Y. Ikeda, T. Inoue, N. Ishii, H. Nemura, K. Sasaki, Are two nucleons bound in lattice QCD for heavy quark masses? Consistency check with Lüscher's finite volume formula, Phys. Rev. D 96 (3) (2017) 034521, https://doi.org/10.1103/PhysRevD.96.034521, arXiv:1703.07210.
[31] T. Iritani, S. Aoki, T. Doi, T. Hatsuda, Y. Ikeda, T. Inoue, N. Ishii, H. Nemura, K. Sasaki, Consistency between Lüscher's finite volume method and HAL QCD method for two-baryon systems in lattice QCD, J. High Energy Phys. 03 (2019) 007, https://doi.org/10.1007/JHEP03(2019)007, arXiv:1812.08539.
[32] B. Hörz, et al., Two-nucleon S-wave interactions at the $SU(3)$ flavor-symmetric point with $m_{ud} \simeq m_s^{\mathrm{phys}}$: a first lattice QCD calculation with the stochastic Laplacian Heaviside method, arXiv:2009.11825, 2020.
[33] T. Iritani, S. Aoki, T. Doi, S. Gongyo, T. Hatsuda, Y. Ikeda, T. Inoue, N. Ishii, H. Nemura, K. Sasaki, Systematics of the HAL QCD potential at low energies in lattice QCD, Phys. Rev. D 99 (1) (2019) 014514, https://doi.org/10.1103/PhysRevD.99.014514, arXiv:1805.02365.
[34] S. Aoki, B. Charron, T. Doi, T. Hatsuda, T. Inoue, N. Ishii, Construction of energy-independent potentials above inelastic thresholds in quantum field theories, Phys. Rev. D 87 (3) (2013) 034512, https://doi.org/10.1103/PhysRevD.87.034512, arXiv:1212.4896.
[35] R.B. Wiringa, R.A. Smith, T.L. Ainsworth, Nucleon nucleon potentials with and without delta (1232) degrees of freedom, Phys. Rev. C 29 (1984) 1207–1221, https://doi.org/10.1103/PhysRevC.29.1207.
[36] S. Okubo, R.E. Marshak, Velocity dependence of the two-nucleon interaction, Ann. Phys. 4 (2) (1958) 166–179.
[37] K. Sasaki, S. Aoki, T. Doi, T. Hatsuda, Y. Ikeda, T. Inoue, N. Ishii, K. Murano, Coupled-channel approach to strangeness $S = -2$ baryon–baryon interactions in lattice QCD, PTEP 2015 (11) (2015) 113B01, https://doi.org/10.1093/ptep/ptv144, arXiv:1504.01717.
[38] C.W. Misner, Spherical harmonic decomposition on a cubic grid, Class. Quantum Gravity 21 (2004) S243–S248, https://doi.org/10.1088/0264-9381/21/3/014, arXiv:gr-qc/9910044.
[39] T. Miyamoto, Y. Akahoshi, S. Aoki, T. Aoyama, T. Doi, S. Gongyo, K. Sasaki, Partial wave decomposition on the lattice and its applications to the HAL QCD method, Phys. Rev. D 101 (7) (2020) 074514, https://doi.org/10.1103/PhysRevD.101.074514, arXiv:1906.01987.
[40] T. Inoue, N. Ishii, S. Aoki, T. Doi, T. Hatsuda, Y. Ikeda, K. Murano, H. Nemura, K. Sasaki, Bound H-dibaryon in flavor SU(3) limit of lattice QCD, Phys. Rev. Lett. 106 (2011) 162002, https://doi.org/10.1103/PhysRevLett.106.162002, arXiv:1012.5928.